

A model-based algorithm for maximum power point tracking of PV systems using exact analytical solution of single-diode equivalent model

Ehsan Moshksar*, Teymoor Ghanbari

School of Advanced Technologies, Shiraz University, Shiraz, Iran

ARTICLE INFO

Keywords:

Analytical approach
Gradient-based algorithm
Irradiance estimation
Model-based MPPT
Parameter estimation

ABSTRACT

A novel model-based technique is presented for maximum power point tracking (MPPT) of photovoltaic (PV) systems. In this paper, an exact single-diode circuit model without any simplification or approximation is considered. Using datasheet information, an adaptive identification technique is utilized to find the electrical parameters uniquely and precisely. After this offline identification scheme, an estimation of solar irradiation is achieved from real-time measurements of PV voltage and current. In the next step, the gradient function of power with respect to voltage is represented from strongly concave mapping between power and voltage. Since the nonlinear gradient consists the complex Lambert W-function, a mathematical formulation is derived to approximate it with conventional logarithmic functions. Finally, a gradient update law is derived to find the unknown optimal voltage value, which results in maximum power generation for any environmental condition. The proposed approach guarantees exponential convergence with highly accurate steady-state performance.

1. Introduction

Maximum power point tracking (MPPT) is an essential approach to promote efficiency of photovoltaic (PV) systems. Extraction of maximum power from PV system in different conditions is relegated to MPPT algorithms. The maximum power is achieved when operating voltage and current remain at the maximum power point (MPP) of the current-voltage ($I-V$) or power-voltage ($P-V$) characteristic curves Ahmed and Salam (2016). An efficient MPPT algorithm can reduce operating cost in addition to increasing efficiency of the overall system Zhang et al. (2015). In general, development of a suitable MPPT algorithm is a challenging task due to the inherent nonlinearity of the problem and its dependency on environmental condition Alajmi et al. (2011). This function is more complicated when solar irradiation and PV temperature have fast variations through time Sera et al. (2008). Therefore, designing a robust and reliable MPPT algorithm with fast operation for uncertain weather condition is crucial in order to harvest more energy from PV modules.

The MPPT algorithms can be classified from different aspects. One of these classifications is related to model-based and model-free approaches (Tang et al., 2016). Perturb and observe (P&O) (Zhang et al., 2013; Kollimalla and Mishra, 2014; Ahmed and Salam, 2016), incremental conductance (Liu et al., 2008; Putri et al., 2015), and extremum-seeking control (Moura and Chang, 2013; Heydari-doostabad et al., 2013; Lauria and Coppola, 2014) are examples of model-free

approaches. These methods only use the measurements of PV voltage and current for determining the MPP without *a priori* knowledge of PV systems. In general the model-free approaches have some disadvantages such as: oscillations around MPP, slow tracking speed, necessity for voltage perturbation, and poor performance in the case of rapidly changing atmospheric conditions (Cristaldi et al., 2014). On the other hand, the model-based MPPT techniques utilize model of PV system or a set of data information to determine MPP. These techniques can overcome many disadvantages of model-free approaches.

The model-based approaches can be classified to analytical and non-analytical methods. The sliding mode control (Zhang et al., 2015), fuzzy logic control (Nabipour et al., 2017), and adaptive neuro-fuzzy inference system (Chikh and Chandra, 2015) are examples of non-analytical methods. These approaches utilize non-direct PV model or a learning procedure to calculate maximum power value. Despite significant advances in nonlinear controller and intelligent approaches, there are few studies on development of effective and reliable analytical methods.

In Xiao et al. (2006), the $P-V$ characteristic is defined explicitly by a set of polynomials. The optimal voltage value at each operating condition is achieved by recursive least-squares and Newton-Raphson methods in real-time. Although this polynomial curve fitting approach results in small oscillation around the MPP, it has considerable computational burden. In addition, this algorithm requires a trade-off between accuracy and complexity. A similar approach has been presented

* Corresponding author.

E-mail addresses: emoshksar@shirazu.ac.ir (E. Moshksar), ghanbarih@shirazu.ac.ir (T. Ghanbari).

in Tsang and Chan (2013), where PV variables are written as polynomial functions of PV voltage, current, and temperature. Orthogonal least squares and forward searching algorithms are applied to solve the MPPT problem. In Rodriguez and Amaratunga (2007), a ball of small radius which also contains the MPP is obtained analytically by mean value theorem. This approach has small oscillation and relatively fast response due to its non-iterative algorithm. However, the final solution has an offset with optimal value because of approximations used in the algorithm. Moreover, no clarification is provided for the case of time-varying weather conditions, especially solar irradiation.

The Gauss-Seidel algorithm has been utilized in Chatterjee et al. (2011) to find the five unknown parameters of the equivalent one-diode electrical circuit model of PV systems. From there, the optimal PV current and voltage are written as functions of equivalent electrical parameters, temperature, and irradiance. This technique is very sensitive to the choice of initial conditions and there is no guarantee for convergence.

An interesting approach is presented in Farivar et al. (2013), where the optimal voltage value expressed as a function of five electrical parameters. The proposed analytic method is simple and fast. However, accuracy of the proposed algorithm highly depends on the values of five unknown parameters. But, no general procedure has given to clear how to estimate these parameters. In Cristaldi et al. (2014), the optimal voltage is defined as a function of PV current, series resistance, and diode thermal voltage. The two electrical parameters are achieved from datasheet information and the optimal current value is obtained from numerical methods. This model-based approach has the advantage of irradiance estimation, but it may suffer from slow performance due to necessity of numeric methods. An optimal voltage control algorithm with fast transient performance and small oscillation, which is suitable for time-varying environmental condition has been presented in Zhao et al. (2015). This algorithm requires the measurements of both solar irradiation and temperature to find MPP value. Moreover, the series and parallel resistances are neglected for finding the analytical solution of optimal voltage value, which may cause bias in final solution.

In this paper, a novel model-based approach is presented for MPPT of photovoltaic systems. The most important step in model-based algorithms is related to the development of an accurate and reliable model for PV module (Cristaldi et al., 2014). However, few researchers have focused on PV model identification for the purpose of maximum power extraction. Therefore, in this work a general process is applied to generate an accurate PV model. First, a single-diode circuit model is considered to predict PV behavior. This model has five unknown parameters in the equivalent circuit. Using the accessible datasheet information, a reduced model with only two unknown parameters is generated as in Laudani et al. (2014). A convex optimization problem and two adaptive update laws are defined to find values of two unknown parameters in the reduced model. Substituting the two obtained values in explicit equations resulted from open circuit, short circuit, and MPP conditions; a unique and precise model is achieved for PV module (Moshksar and Ghanbari, 2017). In the valuable work of Jain and Kapoor (2004), exact analytical solutions are provided for expressing PV output current as function of PV output voltage and vice versa for single-diode model. Although still an exact analytical MPP is difficult to find, simple adaptive update laws can be easily used to solve MPPT problem. First, we have shown that PV output power $P = V \times (I = f(V)) = \ell(V)$ is strictly concave function with respect to voltage. In the next step, the nonlinear function $\frac{d\ell(V)}{dV}$ is derived analytically to find the unknown optimal voltage value in gradient-based algorithm. Since the analytical expression for $\frac{d\ell(V)}{dV}$ consists of complex Lambert W-function, the mathematical approach of Barry et al. (2000) is applied to approximate its principal branch with logarithmic functions. This approximation is not only valid from mathematical perspective, but also for practical implementation of the proposed algorithm. To the best of our knowledge, this is the first model-based

algorithm, which utilizes an exact PV single-diode model to find the maximum power.

One of the main challenges for MPPT is related to dependency of MPP to PV spectral variations (especially for multi-junction devices) and environmental conditions; solar irradiation and temperature (Alajmi et al., 2011). This issue is more controversial in the case of model-based MPPT algorithms. While measuring temperature is a low cost procedure and can be implemented easily, the measurement of solar irradiation requires accurate and expensive pyranometer, which needs to be periodically calibrated (Cristaldi et al., 2012; Mancilla-David et al., 2014). In this work, an estimation of irradiance is achieved form approach presented in Chikh and Chandra (2015), which is based on real-time measurements of PV voltage and current. It is shown that this estimation technique has acceptable result.

The main contributions of this paper can be summarized as follows:

1. Only datasheet information including open circuit voltage, short circuit current, maximum power voltage and current values at standard test condition (STC) are utilized for PV module identification. The five estimated parameters are achieved uniquely without using any approximation in single-diode PV model.
2. A model-based MPPT algorithm is designed according to the identified PV module model. A gradient-based update law is utilized to find optimum voltage value for corresponding weather condition. It is verified that the update law dynamics are stable with adjustable rate of convergence.
3. The proposed model-based MPPT algorithm has an accurate steady-state and transient performance, which is also suitable for MPP under fast time-varying weather condition.
4. The proposed MPPT scheme considers a simple static equation for estimation of solar irradiation using real-time measurements of PV output voltage and current.

The rest of this paper is organized as follows: The procedure to estimate five unknown parameters of PV model is given in Section 2. The MPPT problem formulation is presented in Section 3. The proposed model-based algorithm for MPPT of PV system and its proof of convergence for measurable irradiance and unmeasured irradiance are presented in Section 4. This is followed by simulation and experimental results with some discussions in Section 5. Finally, the summarization of the main results and proof of strongly concavity for mapping between power and voltage of PV module are presented in Sections 6 and A, respectively.

2. PV model identification

The nonlinear I – V characteristic of a PV module with single diode model is given by:

$$I = I_{ph} - I_0 \left[\exp\left(\frac{V + IR_s}{V_t}\right) - 1 \right] - \frac{V + IR_s}{R_p} \quad (1)$$

where I and V are the output current and voltage, respectively. For constant solar irradiation G and module temperature T , the I – V characteristic (1) has five unknown constant parameters as: photocurrent (I_{ph}), diode saturation current (I_0), diode thermal voltage (V_t), series resistance (R_s), and parallel resistance (R_p). R_s and R_p represent the inverse of slope values of I – V curve near open circuit and short circuit conditions, respectively. The relation between diode thermal voltage and diode ideality factor a is given as:

$$V_t = \frac{akTN_s}{q} \quad (2)$$

where k is Boltzmann's constant ($1.3806503 \times 10^{-23}$ J/K), q is electron charge ($1.60217646 \times 10^{-19}$ C), and N_s is the number of series solar cells in a PV module.

Many approaches have been established in order to estimate the five unknown parameters of single diode PV modules (Villalva et al., 2009; Soon and Low, 2012; Khezziar et al., 2014). However, in most of designed approaches, restricted assumptions or approximations are required and the uniqueness of estimated parameters are not guaranteed.

In Moshksar and Ghanbari (2017), a novel approach is presented to estimate the five unknown parameters precisely and uniquely. Based on reduced model in Laudani et al. (2014), we have:

$$R_p = \frac{\phi(R_s, V_t)(R_s I_{sc} - V_{oc}) - V_{mp} - R_s I_{mp} + V_{oc}}{I_{mp} - \phi(R_s, V_t) I_{sc}} = h_1(R_s, V_t) \quad (3)$$

$$I_0 = \frac{I_{sc} - V_{oc}/h_1(R_s, V_t) + R_s I_{sc}/h_1(R_s, V_t)}{\exp(V_{oc}/V_t) - \exp(R_s I_{sc}/V_t)} = h_2(R_s, V_t) \quad (4)$$

$$I_{ph} = \frac{(\exp(V_{oc}/V_t) - 1)(I_{sc} - V_{oc}/h_1(R_s, V_t) + R_s I_{sc}/h_1(R_s, V_t))}{\exp(V_{oc}/V_t) - \exp(R_s I_{sc}/V_t)} + \frac{V_{oc}}{h_1(R_s, V_t)} = h_3(R_s, V_t) \quad (5)$$

where

$$\phi(R_s, V_t) = \frac{\exp(V_{oc}/V_t) - \exp((V_{mp} + R_s I_{mp})/V_t)}{\exp(V_{oc}/V_t) - \exp(R_s I_{sc}/V_t)} \quad (6)$$

The standard test condition values of open-circuit voltage (V_{oc}), short-circuit current (I_{sc}), current (I_{mp}), and voltage (V_{mp}) at the MPP are provided in datasheet information. According to the fact that $\frac{\partial(P=VI)}{\partial V}|_{V_{mp}, I_{mp}} = 0$ and limitations of the physical PV module, an augmented objective function is defined as (Moshksar and Ghanbari, 2017):

$$J(R_s, V_t) = j^2(R_s, V_t) - \mu \sum_{i=1}^3 \ln(\gamma_i(R_s, V_t)) \quad (7)$$

where μ is any positive constant to be assigned and

$$j(R_s, V_t) = (R_s + h_1(R_s, V_t))V_t I_{mp} + (R_s h_1(R_s, V_t)h_2(R_s, V_t)I_{mp} - h_1(R_s, V_t)h_2(R_s, V_t)V_{mp})\exp((V_{mp} + R_s I_{mp})/V_t) - V_t V_{mp} \quad (8)$$

$$\gamma_1(R_s, V_t) = V_t - 0.01285N_s \quad (9)$$

$$\gamma_2(R_s, V_t) = (V_{oc} - V_{mp})/I_{mp} - 3R_s \quad (10)$$

$$\gamma_3(R_s, V_t) = -\ln(I_{sc}/(I_{sc} - I_{mp}))V_t - I_{mp}R_s + V_{oc} - V_{mp} \quad (11)$$

It has been shown in Moshksar and Ghanbari (2017) that the objective function (7) has unique minimizers R_s^* and V_t^* . In order to achieve these unknown minimizers, adaptive parameter update laws are defined as:

$$\hat{R}_s(t) = \begin{cases} -k' \frac{\partial J(\hat{R}_s, \hat{V}_t)}{\partial \hat{R}_s} & \text{if } \hat{R}_s > 2\delta \text{ or } \frac{\partial J}{\partial \hat{R}_s} \leq 0 \\ -k' \frac{\partial J(\hat{R}_s, \hat{V}_t)}{\partial \hat{R}_s} \max\{0, \frac{\hat{R}_s - \delta}{\delta}\} & \text{otherwise.} \end{cases} \quad (12)$$

$$\hat{V}_t(t) = -k' \frac{\partial J(\hat{R}_s, \hat{V}_t)}{\partial \hat{V}_t} \quad (13)$$

where $[\hat{R}_s(t), \hat{V}_t(t)]^T$ is a vector of parameter estimation, $k' > 0$ is a strictly positive constant, and δ is a small positive value. It is proved that $\hat{R}_s(t) \rightarrow R_s^*$ and $\hat{V}_t(t) \rightarrow V_t^*$ at the steady-state. Finally, from substitution of R_s^* and V_t^* in Eqs. (3)–(5), all the five unknown parameters can be achieved at STC.

Generally, the parameters values of PV model can be changed at other environmental conditions. The variations are mostly dependent on irradiance (G) and temperature (T). Photocurrent and diode saturation current for different working conditions are expressed as (Villalva et al., 2009):

$$I_{ph}(G, T) = (I_{ph, ref} + \alpha(T - T_{ref})) \frac{G}{G_{ref}} \quad (14)$$

$$I_0(T) = I_{0, ref} \left(\frac{T}{T_{ref}} \right)^3 \exp \left[\frac{qE_g}{ak} \left(\frac{1}{T_{ref}} - \frac{1}{T} \right) \right] \quad (15)$$

The index ref represents values of different parameters at STC where $G_{ref} = 1000 \text{ W/m}^2$ and $T_{ref} = 298.15 \text{ K}$. E_g is the bandgap energy of the semiconductor which is set to $E_g = 1.12 \text{ eV}$ for polycrystalline silicon cells (Villalva et al., 2009).

The thermal voltage and parallel resistance can be changed with respect to temperature and irradiance, respectively, that is (Ma et al., 2014):

$$V_t(T) = V_{t, ref} \left(\frac{T}{T_{ref}} \right) \quad (16)$$

$$R_p(G) = R_{p, ref} \left(\frac{G_{ref}}{G} \right) \quad (17)$$

To simplify the calculations with an acceptable performance, it can be assumed that series resistance is independent of environmental condition as (Ma et al., 2014):

$$R_s(G, T) = R_s^* \quad (18)$$

3. Problem formulation

The mathematical relation between power, voltage and current of a PV module is defined by:

$$P = V \times I. \quad (19)$$

At any uniform environmental condition, there exists a point (V_{mp}, I_{mp}) such that:

$$P_{mp} = P(V_{mp}, I_{mp}) \geq P(V, I), \forall V \in [0, V_{mp}] \text{ \& } I \in [0, I_{sc}]. \quad (20)$$

The process of finding the optimal point (V_{mp}, P_{mp}) on $P-V$ mapping is known as maximum power point tracking problem. Since the $P-V$ characteristic of a single PV module changes due to variations in solar radiation and module temperature, the values of (V_{mp}, P_{mp}) are varied in the course of time. The $P-V$ characteristics of LG215P1W at different environmental conditions is shown in Fig. 1.

On the other hand, voltage and current in a PV module are highly correlated in a nonlinear manner. Single-diode relation (1), double-diode and triple diode equations are some examples of this correlation. Thus it is possible to have:

$$I = F(V, I). \quad (21)$$

$F(\cdot, \cdot)$ can be any nonlinear function, which is equivalent with $I-V$ curve of a PV module. In general, considering (19) and (21), we have:

$$P = V \times F(V, I) = \ell(V) \quad (22)$$

where nonlinear mapping $\ell(V)$ is a cost function to be maximized. Thus, one can consider the MPPT as static optimization problem in the form:

$$\max_V P = \ell(V). \quad (23)$$

The objective is to bring the input signal V to the unknown maximizer $V^* = V_{mp}$ that maximizes the cost function P . Due to the changes of V_{mp} values with respect to changes in environmental condition, the optimization problem (23) has to be solved in real-time.

4. Model-based MPPT

A novel MPPT algorithm is proposed from the developed model in Section 2. Two different conditions are considered to track the unknown MPP of PV system. First, it is assumed that solar irradiance G and PV temperature T are available for measurement. In the next step, it is assumed that only PV temperature is measurable and solar irradiance G is not available for measurement. Therefore, estimation of irradiance

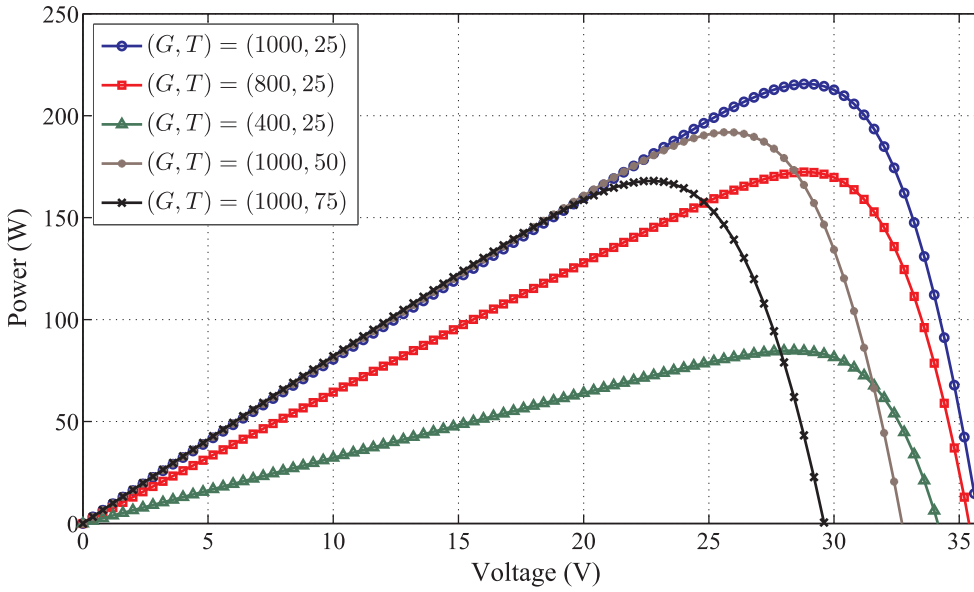


Fig. 1. P–V characteristics at different environmental conditions.

G is accomplished from the real-time measurements of output voltage and output current of PV module.

4.1. Measurable irradiance

The I – V characteristic (1) is a transcendental function and it is not possible to solve it for V in terms of I and vice versa. However, an explicit solution for current can be expressed as follows (Jain and Kapoor, 2004):

$$I = f(V) = -\frac{V}{R_s + R_p} - \frac{W(g(V))V_t}{R_s} + \frac{R_p(I_0 + I_{ph})}{R_s + R_p} \quad (24)$$

where $W(\cdot)$ is Lambert W-function, which is defined by:

$$W(x)\exp(W(x)) = x \quad (25)$$

For real values of $W(\cdot)$, the range of x is limited to $x \geq -\exp(-1)$. The function $W(x)$ has two main branches at real values of x : the principal branch $W_0(x)$ and lower branch $W_{-1}(x)$, where each has many applications in physical systems (Corless et al., 1996). This function is depicted in Fig. 2 for real values of x .

The nonlinear function $g(V)$ is defined as:

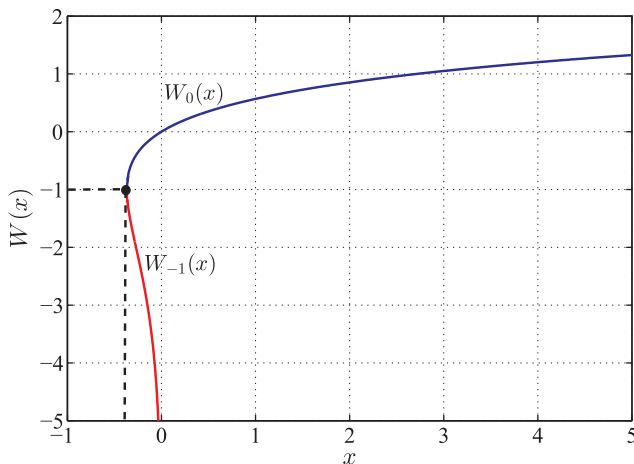


Fig. 2. The two main branches of $W(x)$ function.

$$g(V) = \frac{R_s I_0 R_p \exp\left(\frac{R_p(R_s I_{ph} + R_s I_0 + V)}{V_t(R_s + R_p)}\right)}{V_t(R_s + R_p)} \quad (26)$$

Therefore, The PV output power can be written as:

$$P = V \times I = V \times f(V) = \ell(V) \quad (27)$$

Proposition 1. The nonlinear mapping $P = \ell(V)$ is strongly concave function, i.e., there exists a constant value $\lambda > 0$ such that $\frac{d^2 \ell(V)}{dV^2} \leq -\lambda < 0$ for all admissible values of PV output voltage $V \in [0, V_{oc}]$. Moreover, it is possible to assign $\lambda = \frac{2}{R_s + R_p}$ for a PV module with equivalent single-diode electrical circuit model.

Proof. The proof of Proposition 1 is given in Appendix A.□

Since the nonlinear mapping $P = \ell(V)$ is strongly concave function with respect to voltage, one can consider (27) as a cost function and find the optimum value $V_{mp} = V^*$ that maximize power by utilizing gradient algorithm. For this purpose, the gradient of power with respect to voltage is computed as:

$$\frac{dP}{dV} = \frac{d\ell(V)}{dV} = I + V \times \frac{dI}{dV} = f(V) + V \times \frac{df(V)}{dV} \quad (28)$$

By differentiation of (24) with respect to voltage and substituting in (28), we have:

$$\frac{dP}{dV} = \frac{d\ell(V)}{dV} = f(V) + V \times \left[-\frac{1}{R_s + R_p} - \frac{V_t}{R_s} \times \frac{dW(g(V))}{dV} \right] \quad (29)$$

Based on the chain rule, we obtain:

$$\frac{dW(g(V))}{dV} = \frac{dW}{dg} \times \frac{dg(V)}{dV} \quad (30)$$

where

$$\frac{dW}{dg} = \frac{1}{g(V) + \exp(W(g(V)))} = g_1(V) \quad (31)$$

$$\frac{dg(V)}{dV} = \frac{R_s I_0 R_p^2 \exp\left(\frac{R_p(R_s I_{ph} + R_s I_0 + V)}{V_t(R_s + R_p)}\right)}{V_t^2(R_s + R_p)^2} = g_2(V) \quad (32)$$

Substitution of Eqs. (30)–(32) in (29), results in:

$$\frac{d\ell(V)}{dV} = f(V) - V \times \left[\frac{1}{R_s + R_p} + \frac{V_t}{R_s} g_1(V) g_2(V) \right] \quad (33)$$

Hence, a gradient update law is defined as:

$$\dot{\hat{V}} = k_g \frac{d\ell(\hat{V})}{d\hat{V}} \quad (34)$$

where $k_g > 0$ is an optimization gain.

Theorem 2. In the case of measurable G and T with known parameters of PV module, the update law (34) is such that $\hat{V}(t)$ converges exponentially to the maximizer $V_{mp} = V^*$ of the strongly concave cost function (27). Rate of convergence is adjustable by optimization gain k_g .

Proof. Let $\tilde{V} = \hat{V}(t) - V^*$ and consider the following Lyapunov function candidate:

$$\mathcal{V} = \frac{1}{2} \tilde{V}^2 \quad (35)$$

The time derivative of the Lyapunov function is given by:

$$\dot{\mathcal{V}} = \tilde{V} \dot{\tilde{V}} = k_g \frac{d\ell}{d\hat{V}} \tilde{V}. \quad (36)$$

Since $P = \ell(\hat{V})$ is strongly concave function and $\left. \frac{d\ell(\hat{V})}{d\hat{V}} \right|_{\hat{V}=V^*} = 0$, we have:

$$\frac{d\ell(\hat{V})}{d\hat{V}} (\hat{V} - V^*) \leq -\lambda (\hat{V} - V^*)^2, \forall \hat{V} \in [0, V_{oc}] \quad (37)$$

where $\lambda > 0$ is a constant value such that $\left| \frac{d^2\ell(V)}{dV^2} \right| \geq \lambda$. Substitution of (37) in (36) yields:

$$\dot{\mathcal{V}} = -\lambda k_g \tilde{V}^2 < 0, \hat{V} \neq V^*. \quad (38)$$

The inequality (38) confirms the exponentially convergence of the trajectory $\hat{V}(t)$ to its optimal value V^* . Also, it can be observed from (38) that the rate of convergence depends on the gain k_g . This completes the proof. \square

Considering the gradient of power with respect to voltage in (33), it is clear that the reference voltage update law (34) consists of two Lambert W-functions in $f(V)$ and $g_1(V)$. Since Lambert W-function is not a standard function, it is desirable to approximate it with known standard functions for ease of implementation (Farivar et al., 2013). In this work, the analytical approximation of $W_0(x) \geq 0$ in Barry et al. (2000) is utilized to approximate $W(g(V)) > 0, \forall V \in [0, V_{oc}]$ as:

$$W(x) = (1 + \varepsilon) \ln \left(\frac{\frac{6}{5}x}{\ln \left(\frac{\frac{12}{5}x}{\ln \left(1 + \frac{12}{5}x \right)} \right)} \right) - \varepsilon \ln \left(\frac{2x}{\ln(1 + 2x)} \right) \quad (39)$$

where $\varepsilon = 0.4586887$. The expression (39) is an accurate approximation of $W_0(x) \geq 0$ with the maximum relative error 0.196% as it has been shown in Barry et al. (2000).

4.2. Unmeasured irradiance

Unlike temperature measurement, the direct measurement of solar radiation is difficult and expensive task (Myers, 2005; Carrasco et al., 2014) due to the need of multiple pyranometers and the cost of these solar radiation sensors (Cristaldi et al., 2012). Fortunately, it is possible to estimate the solar irradiance G from the measurements of PV output voltage, output current and temperature (Cristaldi et al., 2014).

In this paper, the estimation of solar irradiance is achieved only by measuring the voltage and current of PV module. First, a reference model is generated for PV module at STC from the approach described

in Section 2. Then, the solar irradiance G at real environmental condition is estimated as (Chikh and Chandra, 2015):

$$G = G_{ref} \left(\frac{I_{sc,ref} + \Delta I}{I_{sc,ref} - \frac{\alpha}{\beta} (R_s \Delta I + \Delta V)} \right) \quad (40)$$

where the constants α and β in datasheet are module's short-circuit current temperature coefficient and open-circuit voltage temperature coefficient, respectively. The changes in module current and voltage due to variations of climatic conditions with respect to their STC values are calculated as (Chikh and Chandra, 2014):

$$\Delta I = I_n - I_{ref} \quad (41)$$

$$\Delta V = V_n - V_{ref} \quad (42)$$

where I_n and V_n are the real measurements of PV module current and voltage at real working condition. Also, I_{ref} and V_{ref} are current and voltage values of PV reference model at STC. When G is estimated, the five parameters of single-diode model are calculated from Eqs. (14)–(17). Finally, the optimal voltage value V_{mp} at real environmental condition can be achieved from the update law (34), where the Lambert W-function is substituted by expression (39). Flowchart of the proposed model-based MPPT algorithm is shown in Fig. 3. The algorithm has three main steps. The first step is an offline approach to estimate the five unknown parameters of single-diode circuit model of PV module and also identify the I – V characteristic at STC. The second step is a real-time approach to estimate solar irradiance from online measurements of PV voltage and current. Also, the values of five parameters are determined at real operating condition of PV system from measured T and estimated G in this step. The key part of the proposed algorithm is step 3, in which the optimal voltage value V_{mp} at real operating condition (G, T) is calculated by the model-based approach in real-time. It is shown that the designed gradient-based reference voltage update law (34) converge exponentially to the unknown V_{mp} value.

Remark 1. It should be noted that the proposed MPPT algorithm is suitable for PV modules that can be effectively described by single-diode equivalent circuit. Otherwise, other equivalent models such as double-diode circuit might be required. Moreover, the proposed model-based MPPT method is only applicable to normal working condition with uniform solar irradiance and PV temperature. The proposed MPPT algorithm is not suitable for partial shading or any anomalous condition. However, its combination with a model-free approach can be applied as an efficient hybrid MPPT technique for global optimization. These topics are out of scope of current paper and they are subjects of future studies.

5. Results and discussions

5.1. Simulation results

To show the performance of the proposed approach, PV module LG215P1W is used for simulation purpose with parameter specifications as: $V_{oc,ref} = 35.8$ V, $I_{sc,ref} = 8.1$ A, $V_{mp,ref} = 28.9$ V, $I_{mp,ref} = 7.46$ A, $N_s = 60$, $\alpha = 0.015$ A/°C and $\beta = -0.323$ V/°C. In order to accomplish the proposed model-based MPPT algorithm, an accurate and reliable PV model is required. First, the offline method of Moshksar and Ghanbari (2017) is used to generate a robust PV model based on the provided parameter specifications. After constructing the convex objective function (7), the parameter update laws (12) and (13) with initial conditions $\hat{R}_s(0) = 0.1$ Ω and $\hat{V}_t(0) = 1.5$ are derived to estimate series resistance and diode thermal voltage, respectively. The result is shown in Fig. 4. The corresponding optimal values are $R_{s,ref} = 0.2526$ Ω and $V_{t,ref} = 1.7983$. It should be noted that convergence speed of this offline method can be made arbitrary fast by adjusting the estimation gains k' and μ . For simulation results of this paper, these gains are chosen as

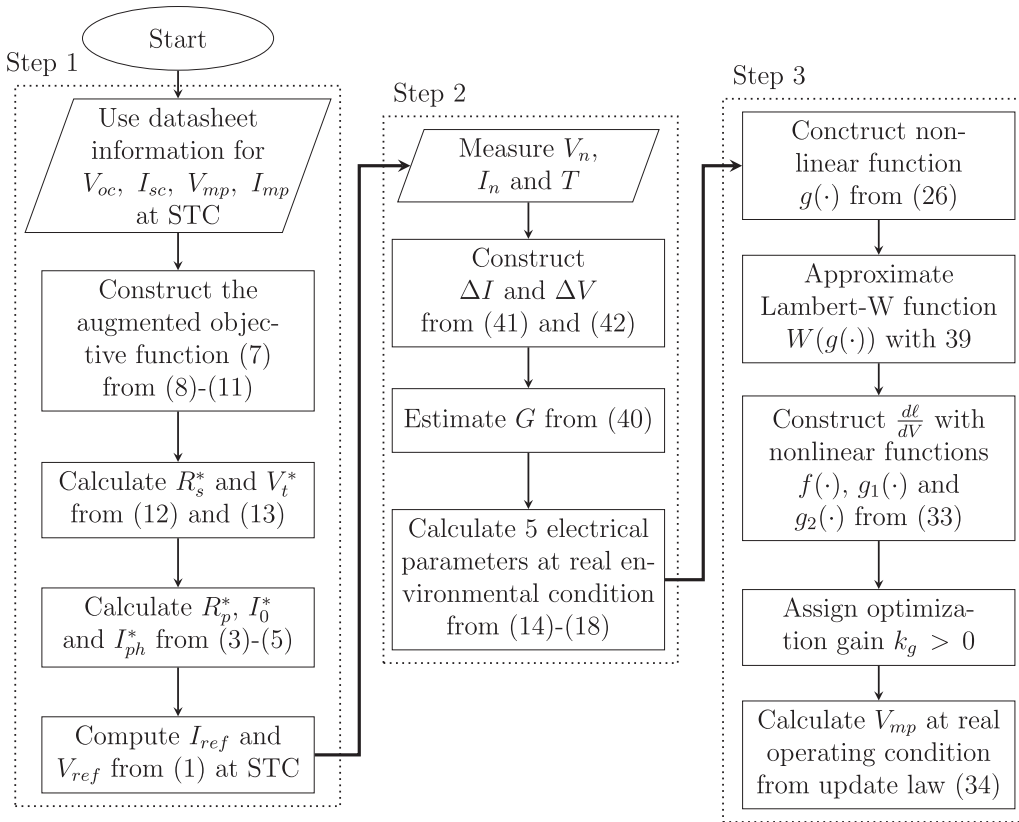


Fig. 3. Flowchart of the proposed model-based MPPT algorithm.

$k' = 50$ and $\mu = 0.1$.

The other three unknown parameters of single-diode PV circuit model are achieved as $R_{p,ref} = 187.85 \Omega$, $I_{0,ref} = 1.791 \times 10^{-8} \text{ A}$ and $I_{ph,ref} = 8.1109 \text{ A}$ from Eqs. (3)–(5) at STC. Since all the five parameters of single-diode PV module are identified, the I – V characteristic of the reference model can be achieved from (1). The I – V reference curve for PV module LG215P1W at STC is shown in Fig. 5.

This model identification technique has advantage of unique

solution for any chosen initial guess. Moreover, the generated PV model is accurate near the MPP, while it is exactly passing through this point (Moshksar and Ghanbari, 2017), as shown in Fig. 5.

The next step is a real-time approach to find the MPP of a PV system in real operating condition. In this paper, a conventional boost converter is utilized and the proposed MPPT algorithm is implemented in its controller. However, any other type of DC-DC converters can be used for voltage regulation, as well. It is assumed that environmental

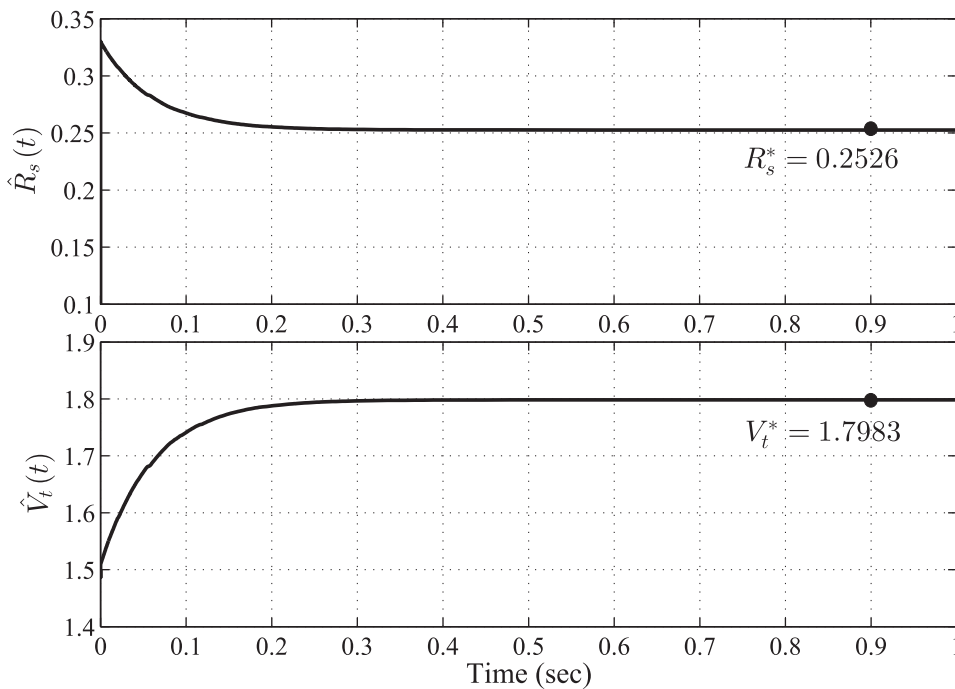


Fig. 4. Series resistance and diode thermal voltage estimation at STC.

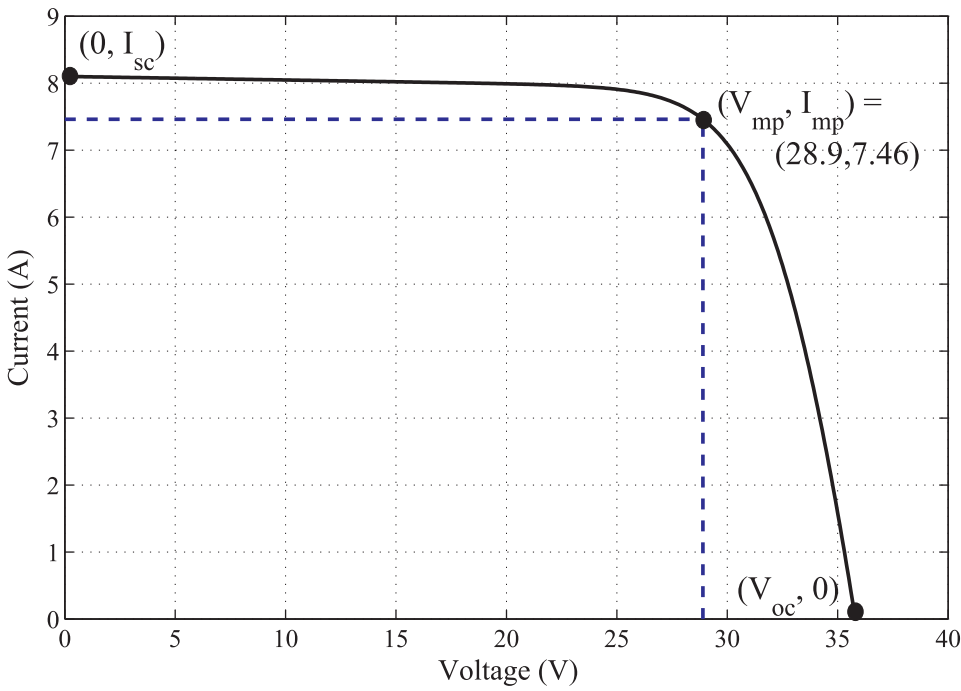


Fig. 5. I – V characteristic of PV module LG215P1W at STC.

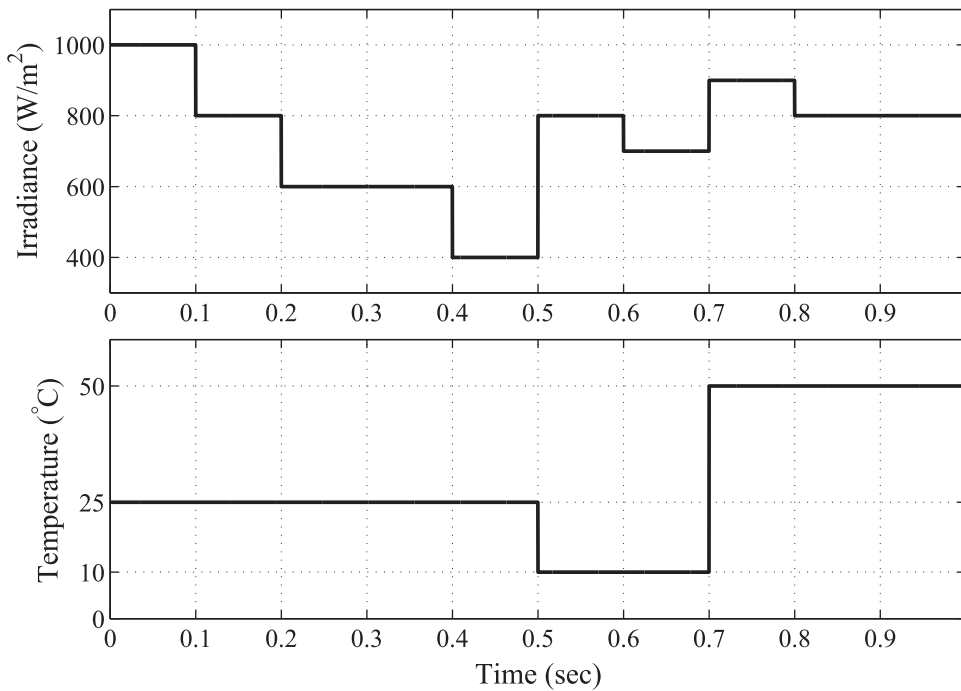


Fig. 6. Time-varying environmental condition pattern.

conditions are changed through time as depicted in Fig. 6.

The temperature T is easy to measure but, a suitable pyranometer may not be available for measurement of irradiance G . In this case, the expression (40) is utilized to estimate solar irradiation. This step is accomplished by measurements of voltage and current of PV module at real operating condition and its comparison with the reference model, achieved from the offline step. Hence, in the case of unmeasured G , measurements of voltage and current are required in order to estimate solar irradiation. The estimated solar trajectory is shown in Fig. 7.

It can be concluded that irradiance estimator (40) does not have uniform performance for all ranges of operating conditions. More specifically, the irradiance estimator (40) has lower accuracy at low irradiances and high temperatures. However, the mean relative error

between the estimated irradiance and its real values at the steady-state for all range of weather conditions is about 1.6%, which is an acceptable value. Also, the maximum relative error is about 3.78% which belongs to $(G, T) = (400, 25)$. From the estimated G and the measured T , the update values for five electrical parameters at real working condition are obtained from Eqs. (14)–(18).

The main step of the proposed real-time algorithm is to find the optimal reference voltage value V^* , which is corresponding with maximum power of PV system derived by the update law (34). The optimization gain k_g dictates the convergence speed to the MPP. In (34), $\frac{dP}{dV}$ is the gradient of power with respect to voltage, achieved from non-linear functions $f(\cdot)$, $g_1(\cdot)$, and $g_2(\cdot)$. The complex Lambert W-function

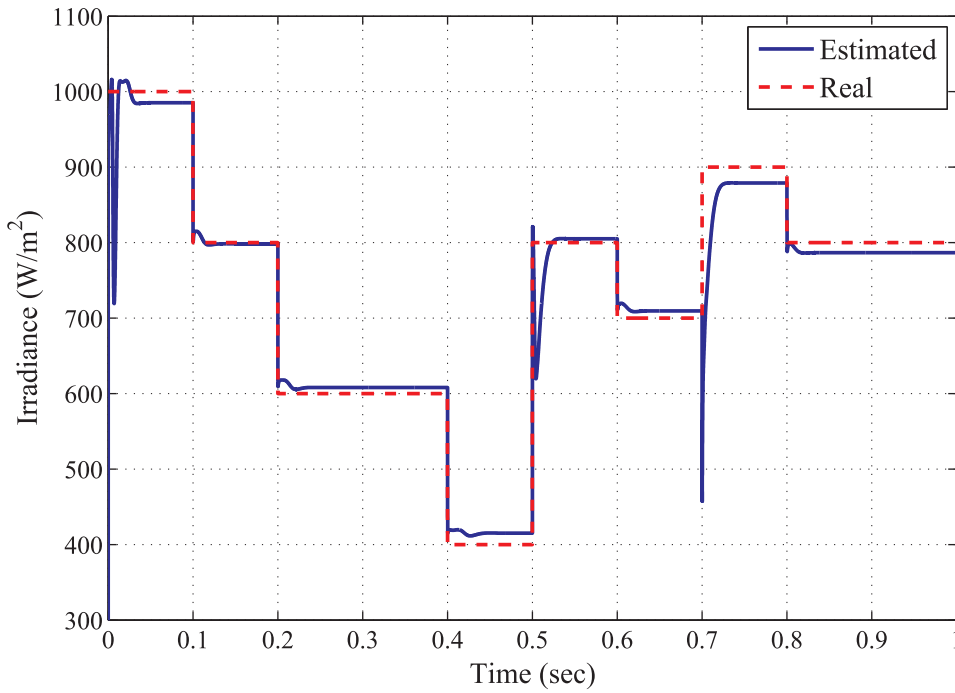


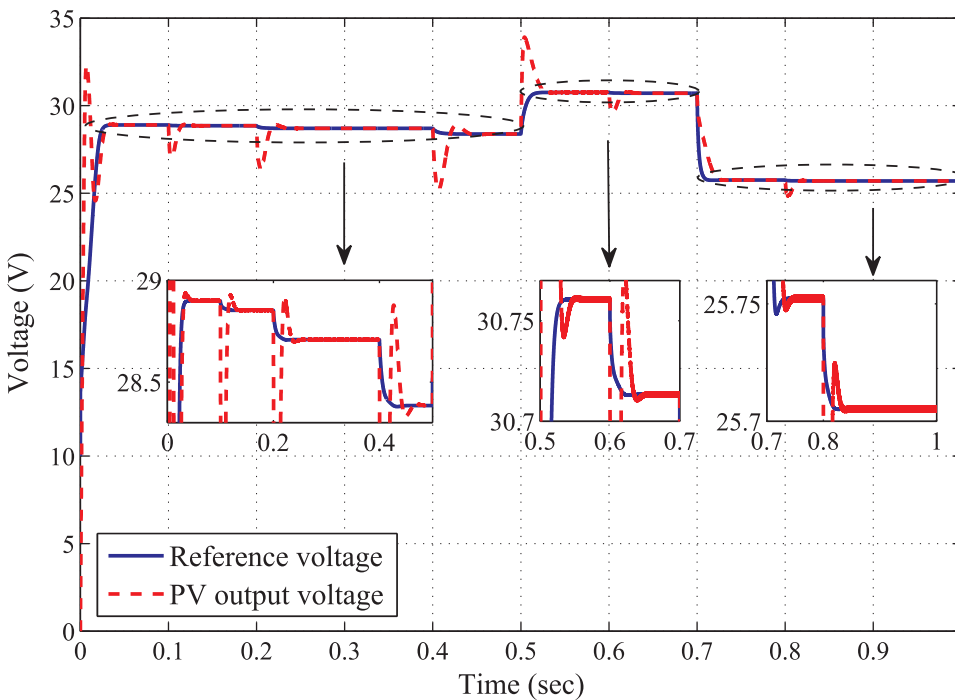
Fig. 7. The trajectory of estimated solar irradiation.

in $f(\cdot)$ and $g(\cdot)$ is approximated by standard $\ln(\cdot)$ function as in (39). Finally, the generated reference voltage value from (34) is subtracted from PV output voltage and the resulted error is applied to a PI controller for generating a suitable duty cycle command for the DC-DC switching converter.

For simulation, the optimization gain is set to $k_g = 100$ and the PI controller has transfer function $PI(s) = P + \frac{1}{s}I$ with $P = 0.005$ and $I = 5$. The simulation results are shown in Figs. 8–10. The trajectories of the reference voltage $\hat{V}(t)$ from update law (34) and PV output voltage $V(t)$ are depicted in Fig. 8. This figure confirms that with designed PI controller, the reference voltage converge to PV output voltage with good transient and steady-state performance.

The output voltage trajectories of the PV system in both cases of

measurable and unmeasured G with the corresponding optimal voltage values are depicted in Fig. 9. As observed from this figure, the voltage trajectories for measured and unmeasured irradiances have very similar behaviors. However, both trajectories have small bias with respect to optimal PV voltage values at different environmental conditions with the exception of STC at time range [0–0.1] seconds. The offset between PV output voltage and its optimal value arises from small mismatch between real values of five parameters of single diode-model and their approximations Eqs. (14)–(18) for different G and T values. In other words, utilizing more reliable and more precise approximations of five model parameters at real environmental condition results in better MPPT performance. Also, the corresponding PV output power trajectories with their maximum values at different operating condition is

Fig. 8. The trajectories of $\hat{V}(t)$ and $V(t)$.

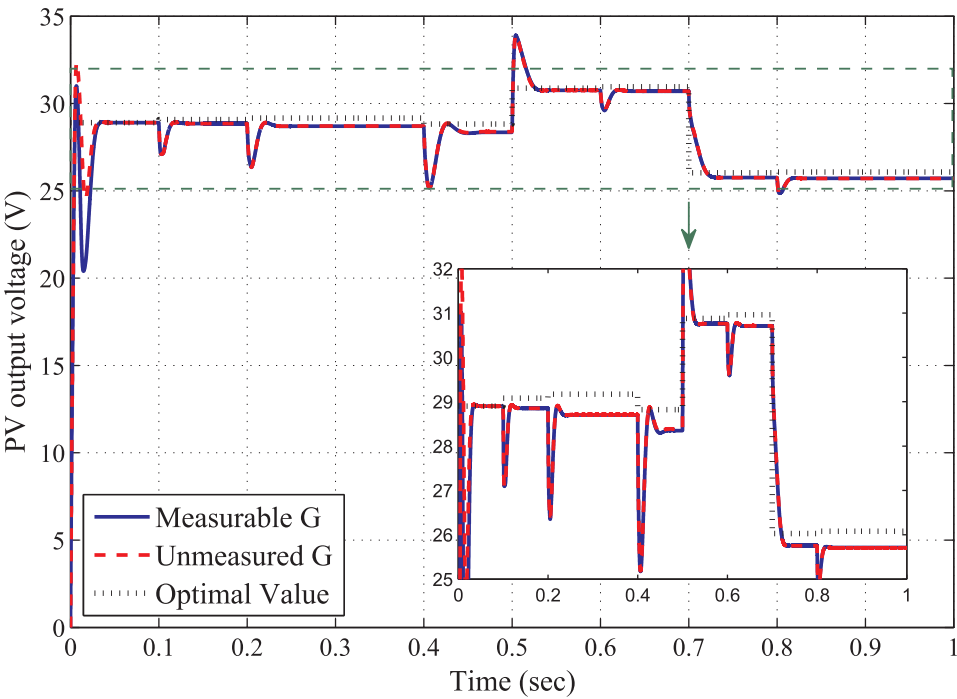


Fig. 9. The trajectories of $V(t)$ for measurable and unmeasured irradiance G .

shown in Fig. 10. Again, it can be seen that PV power trajectory with estimated solar irradiation has similar behavior with the power trajectory resulted from the measured irradiance.

For better insight, the quantitative comparison between measurable and unmeasured irradiance conditions and the corresponding optimal values at different time ranges are shown in Table 1. It is clear that the proposed MPPT algorithm has a very good performance for both measurable and estimated irradiance conditions. The maximum relative errors for PV output voltage and power are 1.631% and 0.501%, respectively. These values belong to time range [0.4–0.5] seconds, where $G = 400 \text{ W/m}^2$ and $T = 25^\circ\text{C}$. From Table 1, it can be concluded that Eqs. (14)–(18) for estimation of five parameters at real environmental condition have less accuracy at lower G and/or higher T . It should be

Table 1
Relative errors for measured and estimated G .

| Time range (s) | Voltage relative error (%) (with G , without G) | Power relative error (%) (with G , without G) |
|----------------|---|---|
| 0–0.1 | (0.002, 0.006) | (0, 0) |
| 0.1–0.2 | (0.757, 0.791) | (0.058, 0.059) |
| 0.2–0.4 | (1.611, 1.577) | (0.227, 0.219) |
| 0.4–0.5 | (1.631, 1.527) | (0.506, 0.449) |
| 0.5–0.6 | (0.390, 0.384) | (0.038, 0.038) |
| 0.6–0.7 | (0.814, 0.795) | (0.009, 0.087) |
| 0.7–0.8 | (1.033, 1.063) | (0.071, 0.075) |
| 0.8–1.0 | (1.402, 1.434) | (0.127, 0.134) |

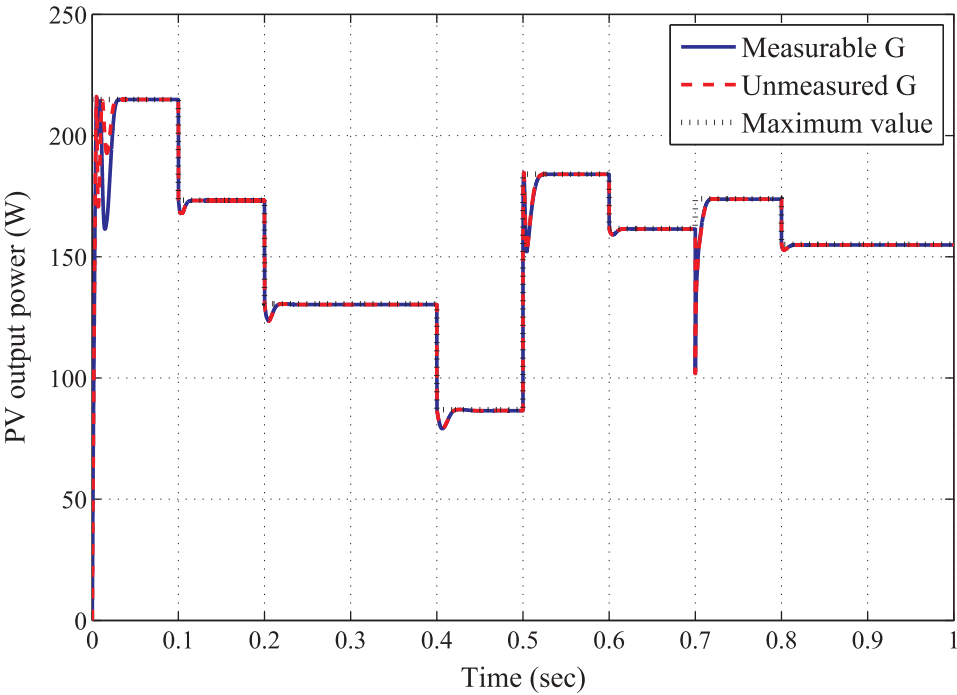


Fig. 10. The trajectories of $P(t)$ for measurable and unmeasured irradiance G .

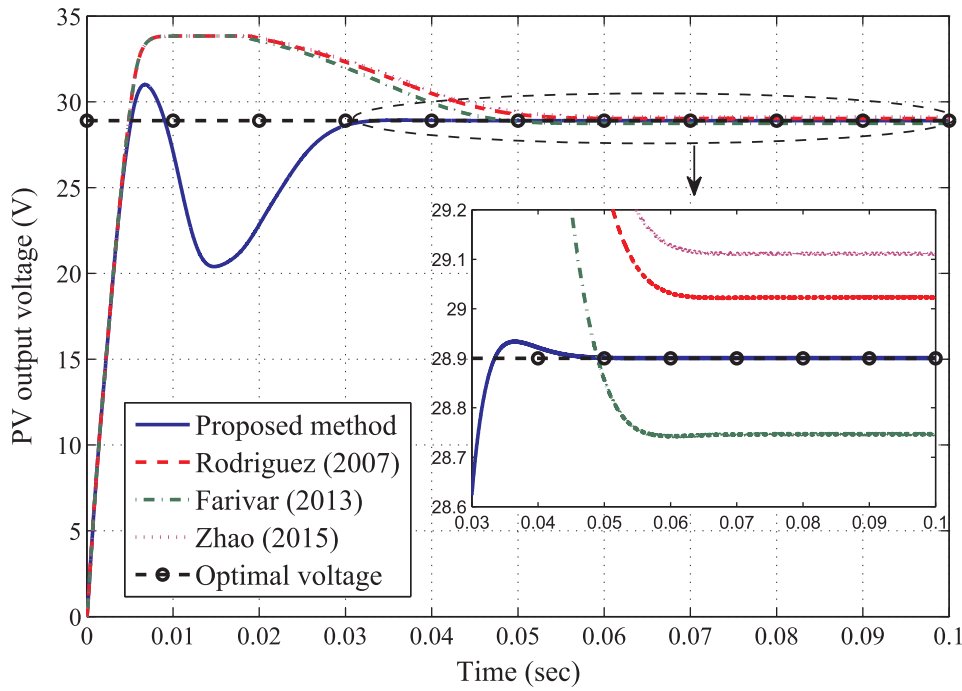


Fig. 11. The trajectories of $V(t)$ for different model-based MPPT methods.

noted that larger error in irradiance estimation with respect to its real value, results in larger error of maximum power estimation for the proposed model-based algorithm.

To indicate accuracy of the generated MPPT algorithm, two different comparisons are presented. First, a comparison is presented between the proposed algorithm and model-based approaches described in Rodriguez and Amaratunga (2007), Farivar et al. (2013), and Zhao et al. (2015). Finally, a comparison is performed between the model-based MPPT technique and conventional P&O algorithm. Since this model-free method is sensitive to the choice of duty cycle's perturbation size, three different ΔD values are considered in simulation results. For sake of comparison, only the STC with $G = 1000 \text{ W/m}^2$ and $T = 25^\circ\text{C}$ is considered because there is no exact information about maximum power value at other weather conditions. A similar PI controller is utilized for all of the compared approaches. Moreover, it is assumed that solar irradiation and temperature are both available for the

Table 2

Comparison of PV voltage relative errors and rate of convergence for different MPPT approaches.

| | Voltage relative error (%) | Settling time (s) |
|---------------------------|----------------------------|-------------------|
| Proposed method | 0.002 | 0.02854 |
| Rodriguez et al. (2007) | 0.429 | 0.04608 |
| Farivar et al. (2013) | 0.535 | 0.044 |
| Zhao et al. (2015) | 0.735 | 0.0467 |
| P&O ($\Delta D = 0.02$) | 0.709 | 0.02902 |
| P&O ($\Delta D = 0.03$) | 0.900 | 0.02094 |
| P&O ($\Delta D = 0.05$) | 1.765 | 0.0139 |

measurements. The PV output voltage trajectories and their corresponding relative error with respect to optimal voltage value $V_{mp} = 28.9 \text{ V}$ at steady-state are shown in Figs. 11 and 12 and Table 2, respectively.

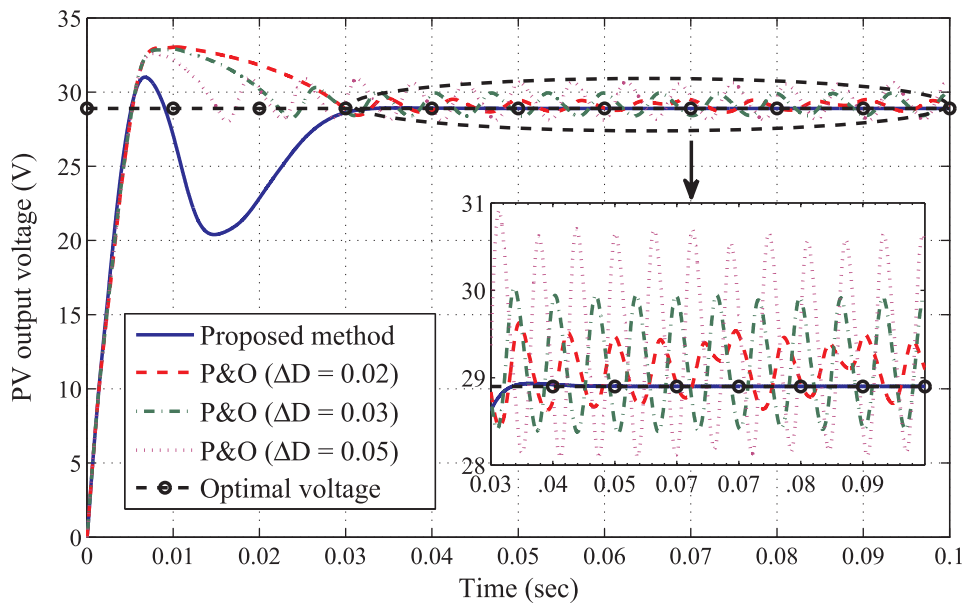


Fig. 12. The trajectories of $V(t)$ for the proposed MPPT algorithm and P&O with different ΔD values.

It can be seen from Fig. 11 that unlike other model-based techniques, the proposed MPPT method exactly converges to its optimal value. Thanks to the employed PV model without any simplification, the proposed method has such more accuracy. In addition, as confirmed in Fig. 11, the proposed algorithm converges to the optimal solution with higher speed. Similarly, Fig. 12 confirms that the proposed model-based MPPT has more precise response compare to P&O algorithm without any oscillation. Although larger ΔD value generates a faster response, it still suffers from high oscillations and loss of the available energy.

Quantitative comparisons are provided in Table 2. For computing relative error of P&O algorithm, the mean value between maximum and minimum oscillation values at steady-state is considered. Also, settling time is computed as the time, where the voltage trajectory reaches to 2% of its final value at the steady-state. It is obvious from Table 2 that the proposed MPPT method has less relative error compared to other MPPT algorithms. Moreover, as it is verified, the precise response of the proposed algorithm achieves in small and acceptable settling time. It should be noted that the speed of algorithm can be increased by increasing the optimization gain k_g .

5.2. Experimental validation

A 10-W PV module with datasheet parameters $V_{oc} = 21.6$ V, $I_{sc} = 0.64$ A, $V_{mp} = 17.6$ V, and $I_{mp} = 0.57$ A is utilized for experimental validation. It should be noted that all the above values are under standard test condition. First, the proposed estimation technique in Section 2 is applied to identify 10-W PV module. The five unknown parameters of PV module are achieved as: $R_{s,ref} = 0.1667 \Omega$, $R_{p,ref} = 1706 \Omega$, $V_{t,ref} = 1.66$, $I_{0,ref} = 1.4 \times 10^{-6}$ A, $I_{ph,ref} = 0.6401$ A. To evaluate the accuracy of the identified PV module, the simulated I – V curve with corresponding experimental data at STC ($G = 1000$ W/m² and $T = 25$ °C) are depicted in Fig. 13.

The normalized root mean square error (NRMSE) between real and simulated PV output current is defined as (Hejri et al., 2014):

$$NRMSE(\%) = \frac{\sqrt{\frac{1}{n} \sum_{i=1}^n (I_{exp} - I_{sim})^2}}{\sqrt{\frac{1}{n} \sum_{i=1}^n I_{exp}^2}} \times 100 \quad (43)$$

where n is the number of measured data, I_{exp} is the experimental current

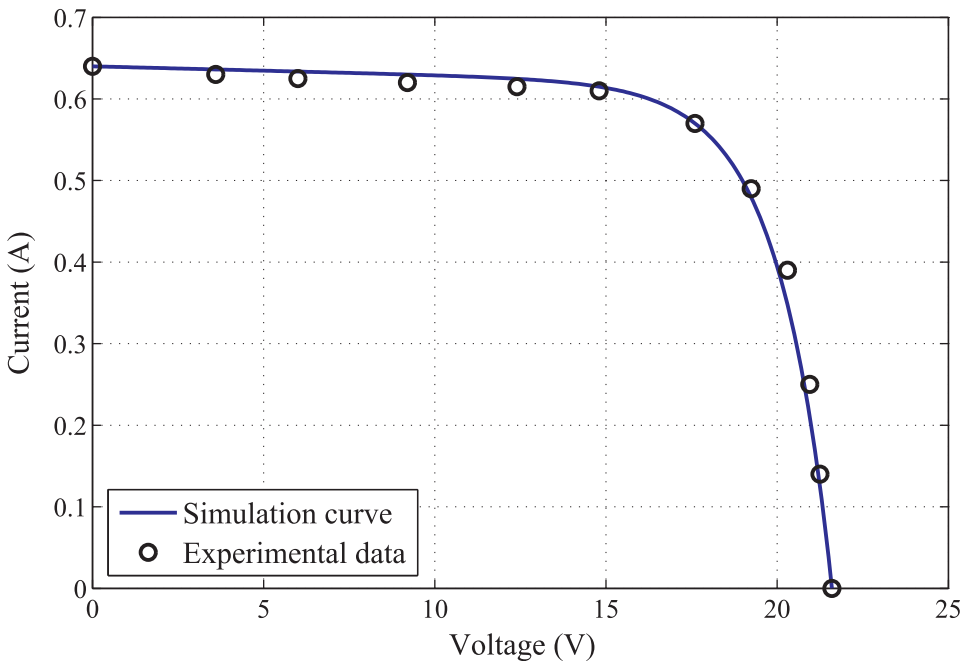


Fig. 13. I – V model curve and experimental data of the 10-W PV module at STC.

and I_{sim} is estimated current from the proposed identification algorithm. The NRMSE(%) value for I – V characteristic in Fig. 13 is around 2.4048%. This small value confirms preciseness of the proposed estimation technique for the purpose of PV model identification.

The aforementioned results for PV module identification were derived as offline. These results are utilized in the proposed model-based MPPT algorithm for real-time extraction of maximum power in practice. The developed experimental setup consists of the 10-W PV module, a DC-DC boost converter, a resistive load, a voltage sensor, and a current sensor. The MPPT technique is implemented by a TMS320F28335 DSP. The 10-W PV panel and experimental test bench are shown in Fig. 14.

Similar to simulation results, a PI controller is employed to regulate PV output voltage. First, the effectiveness of the proposed MPPT controller is verified in start-up condition. To emulate start-up condition, a dark surface placed on the PV panel is removed quickly. The measured temperature is around 38 °C. The relevant experimental results for irradiance estimation are shown in Fig. 15. The PV output voltage and current variations are shown in Figs. 16 and 17. These figures are captured using the digital oscilloscopes.

In order to assess the accuracy of the proposed MPPT in practice, the results are compared with the corresponding derived results from the presented theory. The average value of estimated irradiance at start-up condition is $G = 930.16$ W/m². The calculated MPP value from the theory at this weather condition is $P_{mp} = 8.638$ W and the corresponding value in practice is around $P_{mp} = 8.36$ W. Therefore, there is a small absolute relative error 3.24% between experimental and theory. This small error mostly arises from imperfect relations of Eqs. (14)–(18) for different environmental conditions, inaccuracy of datasheet information, and error in the measurements of PV output voltage and current.

In the previous case study, the performance of the proposed method is assessed in abrupt changing irradiance. Also, the performance of the proposed algorithm in the case of gradually change of solar radiation is evaluated. This condition is emulated by changing the panel orientation, slowly. Typical experimental results for this condition are depicted in Figs. 18–20. As expected, the voltage trajectory in Fig. 19 has small variations because the temperature is almost remained constant ($T \approx 38$ °C).

Similarly, the agreement of theoretical and experimental results is evaluated in the case of time-varying irradiance. Four different solar

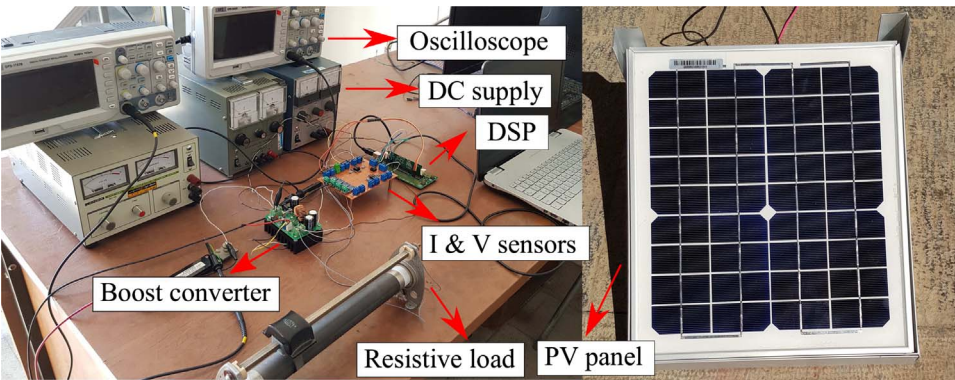


Fig. 14. Photograph of experimental setup.

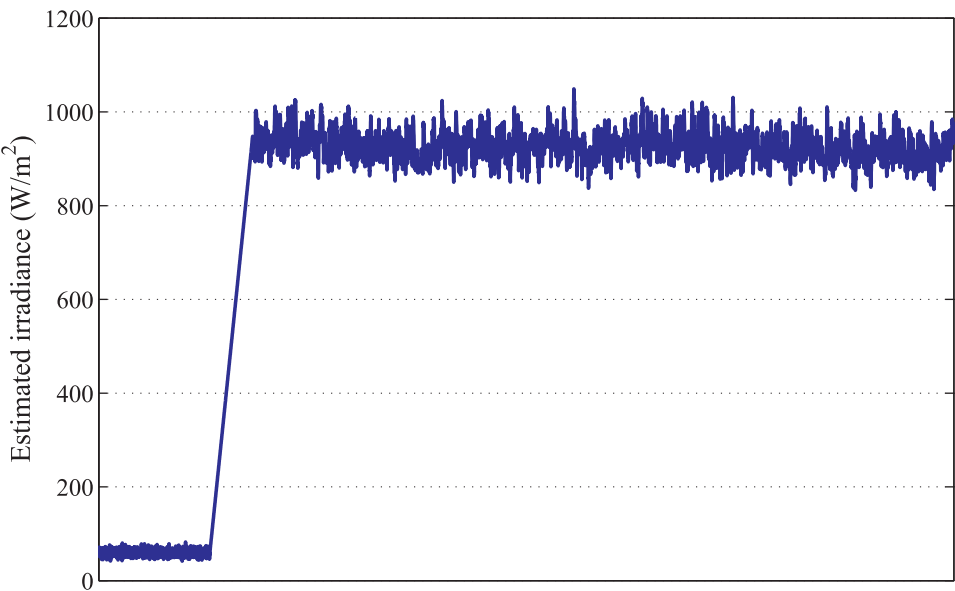


Fig. 15. The trajectory of estimated solar irradiation for start-up condition.

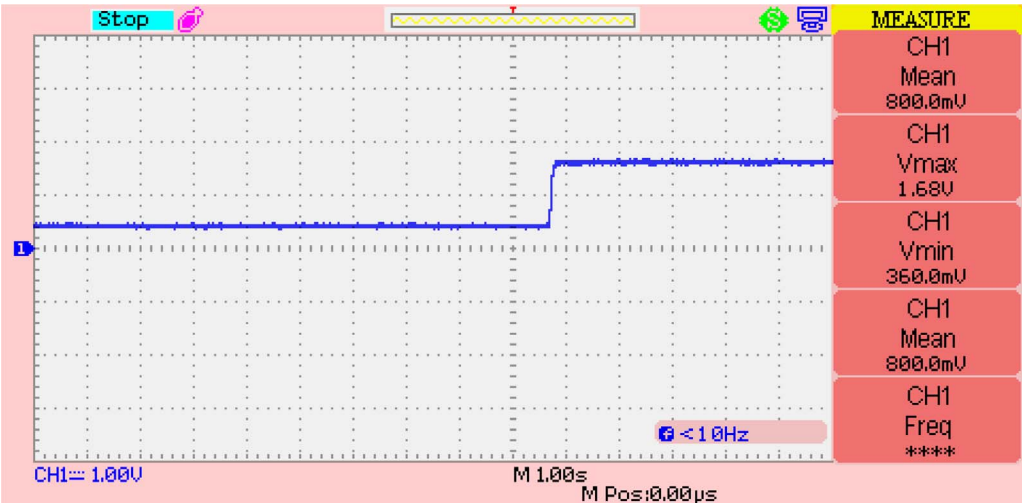


Fig. 16. The trajectory of PV output voltage for start-up condition.

radiation values are chosen from Fig. 18. The theoretical and experimental MPP values at these amounts of solar radiation and for $T = 38^\circ\text{C}$ are calculated and the results are shown in Table 3.

It is clear from Table 3 that the experimental results relevant to higher solar radiations have more agreement with the theory, due to accuracy of Eqs. (14)–(18) at high irradiance. In general, the

experimental results agree well with the corresponding results from presented theory. In addition, the PV power is able to follow the reference values under time-varying solar radiation.

Obviously, the real-time calculation of approximated Lambert W-function (39) is the most time-consuming part of the proposed model-based algorithm. Although the convergence of MPP to its reference

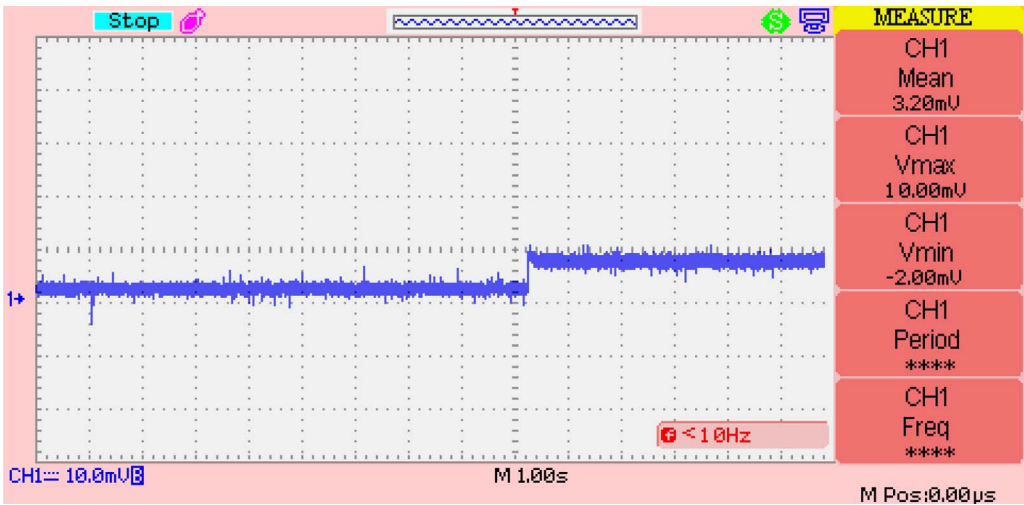


Fig. 17. The trajectory of PV output current for start-up condition.

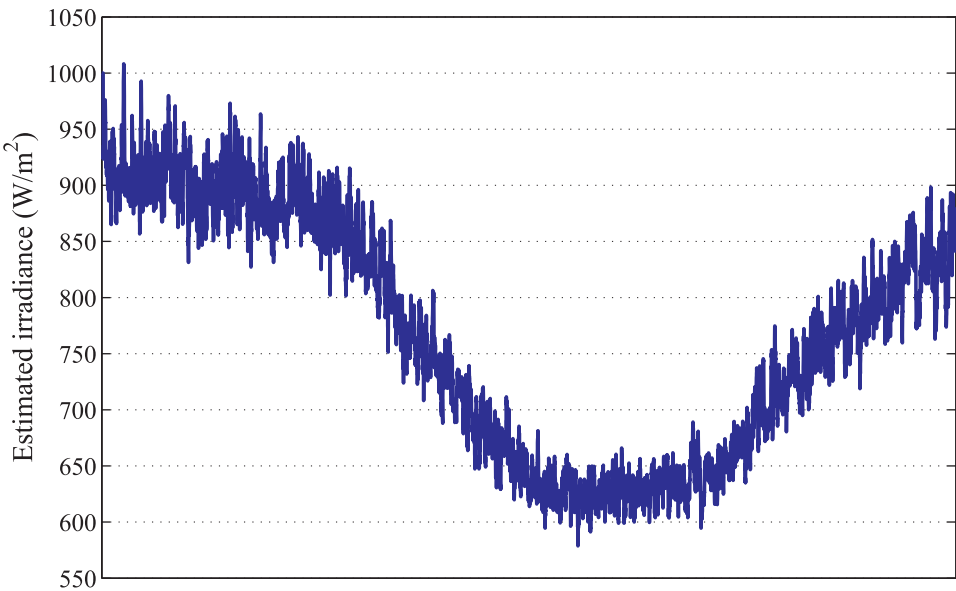


Fig. 18. The trajectory of estimated solar irradiation for variable irradiance.

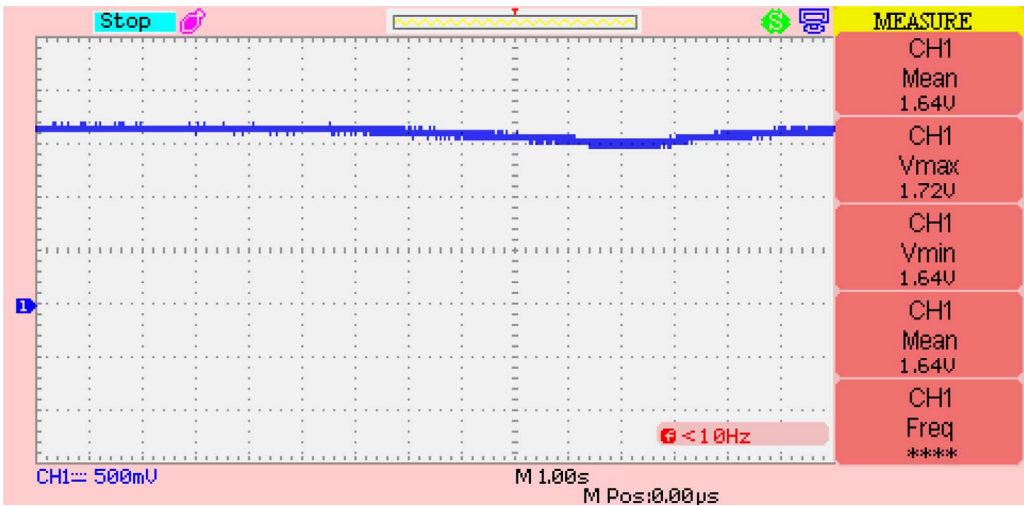


Fig. 19. The trajectory of PV output voltage for variable irradiance.

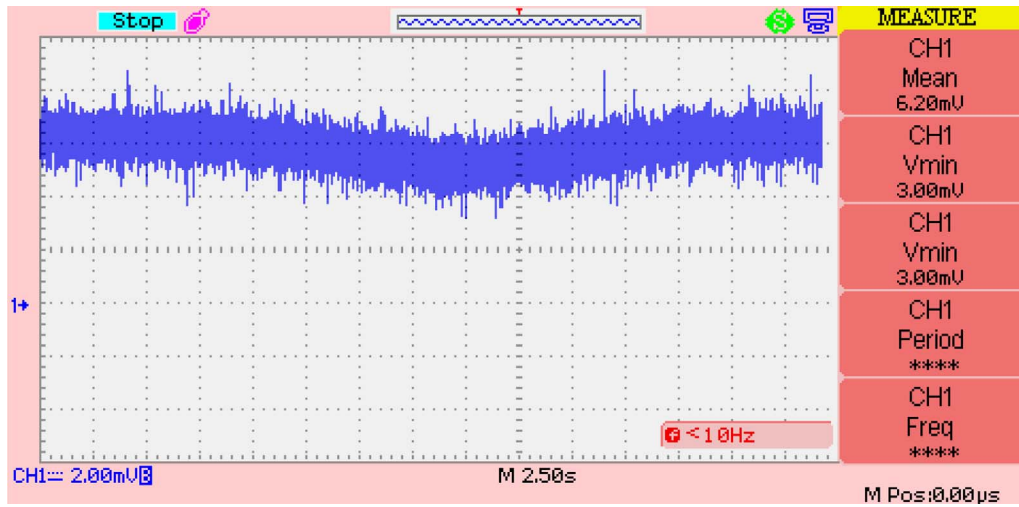


Fig. 20. The trajectory of PV output current for variable irradiance.

Table 3

Comparison of MPP values for theoretical and experimental results at different G values and $T = 38^\circ\text{C}$.

| Irradiance (W/m^2) | 915 | 825 | 735 | 630 |
|--------------------------------------|-------|-------|-------|-------|
| Theoretical MPP value (W) | 8.485 | 7.571 | 6.658 | 5.624 |
| Experimental MPP value (W) | 8.19 | 7.24 | 6.30 | 5.28 |
| Power relative error (%) | 3.48 | 4.37 | 5.38 | 6.11 |

value is satisfactory in the proposed MPPT controller, one can increase the speed of response by utilizing a lookup table instead of relation (39). However, a precise lookup table requires more additional memory space than the presented simple approximated Lambert W-function Farivar et al. (2013).

6. Conclusions

A model-based MPPT algorithm is designed to obtain maximum power from PV systems under different environmental conditions. First, a single diode electrical circuit model is considered as equivalent photovoltaic model. Since this model has five unknown parameters, a novel convex optimization approach is applied to estimate unknown parameters uniquely and precisely. Next, it is shown by rigorous mathematical analysis that the exact analytical relation between power and voltage of single diode PV module generates strongly concave

function. Thanks to the exact and accurate obtained PV model and the strongly concave cost function, any model-based optimization algorithm can be implemented to find optimal value of power. In this paper, the basic gradient update law is proposed to find the unknown optimal PV voltage and its corresponding power value. Since the gradient update law consists of complex Lambert W-function, an explicit equation with logarithmic functions is employed to approximate this function. This approximation is a great advantage for practical implementation of the proposed MPPT algorithm with a DSP. Also, the proposed algorithm has advantage of irradiance estimation from measurements of PV voltage and current in the case that precise pyranometer is not available. This real-time scheme is able to track maximum power in the case of fast weather variations. The proof of convergence to the optimal voltage value is provided for the proposed real-time MPPT solver. It is shown that the steady-state error in this approach is lower than other similar model-based techniques. Moreover, the resulted trajectory from update law dynamics has acceptable transient performance. Simulation and experimental results are presented to confirm effectiveness of the proposed approach.

Acknowledgments

The authors would like to acknowledge the financial support from the National Elites Foundation of Iran.

Appendix A. Proof of Proposition 1

The Hessian function $\frac{d^2\ell(V)}{dV^2}$ is achieved from differentiating (33) with respect to voltage as:

$$\frac{d^2\ell(V)}{dV^2} = \frac{df(V)}{dV} - \left[\frac{1}{R_s + R_p} + \frac{V_t}{R_s} g_1(V) g_2(V) \right] - V \times \frac{V_t}{R_s} \left(g_1(V) \frac{dg_2(V)}{dV} + \frac{dg_1(V)}{dV} g_2(V) \right) \quad (\text{A.1})$$

By differentiating (24), (31), and (32) with respect to voltage and some rearrangements, we have:

$$\frac{df(V)}{dV} = -\frac{1}{R_s + R_p} - \frac{V_t}{R_s} g_1(V) g_2(V) \quad (\text{A.2})$$

$$\frac{dg_1(V)}{dV} = -g_1^2(V) g_2(V) - g_1^3(V) g_2(V) \exp(W(g(V))) \quad (\text{A.3})$$

$$\frac{dg_2(V)}{dV} = \frac{R_p}{V_t(R_s + R_p)} g_2(V) = \frac{R_p^2}{V_t^2(R_s + R_p)^2} g(V) \quad (\text{A.4})$$

Substituting (A.2)–(A.4) in (A.1), one obtains:

$$\frac{d^2\ell(V)}{dV^2} = 2 \frac{df(V)}{dV} - \frac{V_t \times V}{R_s} g_1(V) g_2(V) \left(\frac{R_p}{V_t(R_s + R_p)} - g_1(V) g_2(V) - g_1^2(V) g_2(V) \exp(W(g(V))) \right) \quad (\text{A.5})$$

where $\frac{df}{dV} < 0$ and $g_1(V), g_2(V), g(V) > 0, \forall V \in [0, V_{oc}]$. From (31) and (A.4), the relation between $g_1(V)$ and $g_2(V)$ is expressed as:

$$g_1(V) = \frac{1}{\frac{V_i(R_s + R_p)}{R_p} g_2(V) + \exp\left(W\left(\frac{V_i(R_s + R_p)}{R_p} g_2(V)\right)\right)} \quad (\text{A.6})$$

Therefore, $g_1(V)g_2(V)$ can be written as follows:

$$g_1(V)g_2(V) = \frac{g_2(V)}{\frac{V_i(R_s + R_p)}{R_p} g_2(V) + \exp\left(W\left(\frac{V_i(R_s + R_p)}{R_p} g_2(V)\right)\right)} = \mathcal{F}(g_2(V)) \quad (\text{A.7})$$

Since the nonlinear functions $\mathcal{F}(\cdot)$ and $g_2(\cdot)$ are strictly increasing with respect to their arguments, $\mathcal{F}(g_2(V))$ achieves its maximum value as $V \rightarrow V_{oc}$. By substituting $V = V_{oc}$ and the values of five parameters for the equivalent circuit model of PV module LG215P1W from Section 5, we have:

$$\begin{aligned} R_p/(V_i(R_s + R_p)) &= 0.555 \\ g_1(V)g_2(V) &= 0.2923 \\ g_1^2(V)g_2(V)\exp(W(g(V))) &= 0.1384 \end{aligned} \quad (\text{A.8})$$

From substitution of (A.8) in (A.5) and strictly negativeness of $\frac{df(V)}{dV}$, it is clear that $\frac{d^2\ell(V)}{dV^2} < 0, \forall V \in [0, V_{oc}]$.

In addition, $g_1(0)g_2(0) \approx g_2(0) = \varepsilon' < I_0$. Hence, ε' is a very small value. Considering $\lambda = \min \left| \frac{d^2\ell(V)}{dV^2} \right|$ and Hessian (A.5), it is easy to show that:

$$\left| \frac{d^2\ell(V)}{dV^2} \right| \geq \left| \frac{d^2\ell(V)}{dV^2} \right|_{V=0} = \frac{2}{R_s + R_p} + \frac{2V_i\varepsilon'}{R_s} > \frac{2}{R_s + R_p} = \lambda. \quad (\text{A.9})$$

This completes the proof.

References

- Ahmed, J., Salam, Z., 2016. A modified P&O maximum power point tracking method with reduced steady-state oscillation and improved tracking efficiency. *IEEE Trans. Sust. Energy* 7, 1506–1515.
- Alajmi, B.N., Ahmed, K.H., Finney, S.J., Williams, B.W., 2011. Fuzzy-logic-control approach of a modified hill-climbing method for maximum power point in microgrid standalone photovoltaic system. *IEEE Trans. Power Electron.* 26, 1022–1030.
- Barry, D.A., Parlange, J.Y., Li, L., Prommer, H., Cunningham, C.J., Stagnitti, F., 2000. Analytical approximations for real values of the Lambert W -function. *Math. Comput. Simul.* 53, 95–103.
- Carrasco, M., Mancilla-David, F., Ortega, R., 2014. An estimator of solar irradiance in photovoltaic arrays with guaranteed stability properties. *IEEE Trans. Ind. Electron.* 61, 3359–3366.
- Chatterjee, A., Keyhani, A., Kapoor, D., 2011. Identification of photovoltaic source models. *IEEE Trans. Energy Convers.* 26, 883–889.
- Chikh, A., Chandra, A., 2014. Adaptive neuro-fuzzy based solar cell model. *IET Renew. Power Gener.* 8, 679–686.
- Chikh, A., Chandra, A., 2015. An optimal maximum power point tracking algorithm for PV systems with climatic parameters estimation. *IEEE Trans. Sust. Energy* 6, 644–652.
- Corless, R.M., Gonnet, G.H., Hare, D.E.G., Jeffrey, D.J., Knuth, D.E., 1996. On the Lambert W function. *Adv. Comput. Math.* 5, 329–359.
- Cristaldi, L., Faifer, M., Ponci, F., Rossi, M., 2012. A simple photovoltaic panel model: characterization procedure and evaluation of the role of environmental measurements. *IEEE Trans. Instrum. Meas.* 61, 2632–2641.
- Cristaldi, L., Faifer, M., Rossi, M., Toscani, S., 2014. An improved model-based maximum power point tracker for photovoltaic panels. *IEEE Trans. Instrum. Meas.* 63, 63–71.
- Farivar, G., Asaei, B., Mehrnami, S., 2013. An analytical solution for tracking photovoltaic module MPP. *IEEE J. Photovolt.* 3, 1053–1061.
- Hejri, M., Mokhtari, H., Azizian, M.R., Ghandhari, M., Söder, L., 2014. On the parameter extraction of a five-parameter double-diode model of photovoltaic cells and modules. *IEEE J. Photovolt.* 4, 915–923.
- Heydari-doostabad, H., Keypour, R., Khalghani, M.R., Khooban, M.H., 2013. A new approach in MPPT for photovoltaic array based on extremum seeking control under uniform and non-uniform irradiances. *Solar Energy* 94, 28–36.
- Jain, A., Kapoor, A., 2004. Exact analytical solutions of the parameters of real solar cells using Lambert W -function. *Solar Energy Mater. Solar Cells* 81, 269–277.
- Khezzer, R., Zereg, M., Khezzer, A., 2014. Modeling improvement of the four parameter model for photovoltaic modules. *Solar Energy* 110, 452–462.
- Kollimalla, S.K., Mishra, M.K., 2014. Variable perturbation size adaptive P&O MPPT algorithm for sudden changes in irradiance. *IEEE Trans. Sust. Energy* 5, 718–728.
- Laudani, A., Riganti-Fulginei, F., Salvini, A., 2014. Identification of the one-diode model for photovoltaic modules from datasheet values. *Solar Energy* 108, 432–446.
- Lauria, D., Coppola, M., 2014. Design and control of an advanced PV inverter. *Solar Energy* 110, 533–542.
- Liu, F., Duan, S., Liu, F., Liu, B., Kang, Y., 2008. A variable step size INC MPPT method for PV systems. *IEEE Trans. Ind. Electron.* 55, 2622–2628.
- Ma, T., Yang, H., Lu, L., 2014. Development of a model to simulate the performance characteristics of crystalline silicon photovoltaic modules/strings/arrays. *Solar Energy* 100, 31–41.
- Mancilla-David, F., Riganti-Fulginei, F., Laudani, A., Salvini, A., 2014. A neural network-based low-cost solar irradiance sensor. *IEEE Trans. Instrum. Meas.* 63, 583–591.
- Moshksar, E., Ghanbari, T., 2017. Adaptive estimation approach for parameter identification of photovoltaic modules. *IEEE J. Photovolt.* 7, 614–623.
- Moura, S.J., Chang, Y.A., 2013. Lyapunov-based switched extremum seeking for photovoltaic power maximization. *Control Eng. Pract.* 21, 971–980.
- Myers, D.R., 2005. Solar radiation modeling and measurements for renewable energy applications: data and model quality. *Energy* 30, 1517–1531.
- Nabipour, M., Razaz, M., Seifossadat, S.G., Mortazavi, S.S., 2017. A new MPPT scheme based on a novel fuzzy approach. *Renew. Sust. Energy Rev.* 74, 1147–1169.
- Putri, R.I., Wibowo, S., Rifa'i, M., 2015. Maximum power point tracking for photovoltaic using incremental conductance method. In: *International Conference on Sustainable Energy Engineering and Application*, Energy Procedia. Bandung, Indonesia, pp. 22–30.
- Rodriguez, C., Amaratunga, G.A.J., 2007. Analytic solution to the photovoltaic maximum power point problem. *IEEE Trans. Circ. Syst. I: Reg. Papers* 54, 2054–2060.
- Sera, D., Teodorescu, R., Hantschel, J., Knoll, M., 2008. Optimized maximum power point tracker for fast-changing environmental conditions. *IEEE Trans. Ind. Electron.* 55, 2629–2637.
- Soon, J.J., Low, K.S., 2012. Photovoltaic model identification using particle swarm optimization with inverse barrier constraint. *IEEE Trans. Power Electron.* 27, 3975–3983.
- Tang, R.L., Wu, Z., Fang, Y.J., 2016. Maximum power point tracking of large-scale photovoltaic array. *Solar Energy* 134, 503–514.
- Tsang, K.M., Chan, W.L., 2013. Model based rapid maximum power point tracking for photovoltaic systems. *Energy Convers. Manage.* 70, 83–89.
- Villalva, M.G., Gazoli, J.R., Filho, E.R., 2009. Comprehensive approach to modeling and simulation of photovoltaic arrays. *IEEE Trans. Power Electron.* 24, 1198–1208.
- Xiao, W., Lind, M.G.J., Dunford, W.G., Capel, A., 2006. Real-time identification of optimal operating points in photovoltaic power systems. *IEEE Trans. Ind. Electron.* 53, 1017–1026.
- Zhang, F., Maddy, J., Premier, G., Guwy, A., 2015. Novel current sensing photovoltaic maximum power point tracking based on sliding mode control strategy. *Solar Energy* 118, 80–86.
- Zhang, F., Thanapalan, K., Procter, A., Carr, S., Maddy, J., 2013. Adaptive hybrid maximum power point tracking method for a photovoltaic system. *IEEE Trans. Energy Convers.* 28, 353–360.
- Zhao, J., Zhou, X., Ma, Y., Liu, W., 2015. A novel maximum power point tracking strategy based on optimal voltage control for photovoltaic systems under variable environmental conditions. *Solar Energy* 122, 640–649.